PHYSICAL REVIEW A VOLUME 51, NUMBER 1 JANUARY 1995

Isotope shift in the electron affinity of chlorine

U. Berzinsh,* M. Gustafsson, D. Hanstorp, A Klinkmüller, U. Ljungblad, and A.-M. Mårtensson-Pendrill
Department of Physics, Chalmers University of Technology, S-412 96 Göteborg, Sweden
and Göteborg University, S-412 96 Göteborg, Sweden

(Received 14 July 1994)

The specific mass shift in the electron affinity between ^{35}Cl and ^{37}Cl has been determined by tunable-laser photodetachment spectroscopy to be $-0.51(14)$ GHz. The isotope shift was observed as a difference in the onset of the photodetachment process for the two isotopes. In addition, the electron affinity of Cl was found to be 29 138.59(22) cm^{-1}, giving a factor of 2 improvement in the accuracy over earlier measurements. Many-body calculations including lowest-order correlation effects demonstrate the sensitivity of the specific mass shift and show that the inclusion of higher-order correlation effects would be necessary for a quantitative description.

PACS number(s): 35.10.Hn, 32.80.Fb, 31.30.Gs

I. INTRODUCTION

Tunable-laser photodetachment spectroscopy makes high-resolution studies of electron affinities possible, and in this work we demonstrate an application of this technique to the measurement of the isotope shift in the electron affinity of chlorine. The observed shift is only a fraction of the *normal mass shift* (NMS), indicating a *specific mass shift* (SMS) comparable to the normal mass shift, but of opposite sign. The results obtained provide a sensitive probe of electron correlation effects, which are known to be particularly important, both for negative ions and for the specific mass shift.

The outermost electron in a negative ion is very weakly bound: Far from the nucleus it is bound only due to polarization of the other electrons in the system, whereas the outermost electron in an atom or a positive ion is bound in a long-range Coulomb potential. Hence the electron correlation is of greater importance in negative ions, which therefore provide good tests of computational methods used to describe electron correlation. In Li$^-$, e.g., the electron correlation energy has been found to be three times larger than the electron affinity [1]. Another system where the electron correlation is dominating the binding energy is the two-electron system H$^-$, which has been used as a model case in many calculations [2–4].

The specific mass shift arises from a correlation between the electronic momenta through the motion of the nucleus with its finite mass, and is discussed in more detail in Sec. III A. Being a two-particle operator the SMS is very sensitive to correlation effects, and its calculation is a challenge for atomic theory. The development of methods to include all-order correlation effects on the SMS is in progress, but to our knowledge no calculation has yet been performed for a many-electron system. Inclusion of the lowest-order correlation terms in atomic many-body perturbation theory has been found to give a significant—albeit insufficient—improvement in several cases [5–7] and is here applied to the electron affinity of chlorine, as described in Sec. III.

Since electron correlation is of major importance both for negative ions and for the specific mass shift, it would be of particular interest to investigate the specific mass shift in negative ions. However, the only one experiment, so far, where an isotope effect has been studied in an atomic negative ion is the measurement by Lykke *et al.* [8] of the electron affinities of hydrogen and deuterium. For these light systems, the mass shift is, of course, very large, which enabled Lykke *et al.* to observe a shift, although the outgoing electron is a p wave, resulting in a slow onset of the photodetachment process. The main reason for the lack of studies of isotope shifts in negative ions is the absence of bound excited states which are optically accessible. The only sharp structure in an optical spectrum is the onset of the photodetachment process, and for most negative ions, this threshold is in a wavelength region not accessible to tunable dye lasers. Schulz *et al.* [9] have applied high-resolution techniques to study isotope effects in the negative *molecular* ions OH$^-$ and OD$^-$, where, however, the major part of the mass effect is due to vibration and rotation and not from the electronic part, as in the case of atomic systems.

This work presents an investigation of the isotope shift of chlorine, which was chosen for several reasons. From an experimental point of view, Cl has the advantage, shared with all halogens, that an s electron is emitted in the photodetachment, giving a sharp threshold. In addition, it has two stable isotopes with large natural abundances. From a theoretical point of view, the closed-shell ground state of a halogen ion provides a convenient reference state for the calculations, and makes the system relatively easy to treat. In addition, the specific mass shift in the ionization potential of the rare gases, which involve the same electron configurations, have previously been investigated, theoretically as well as experimentally [10–12], and the comparison of results can give indications about the importance of various effects.

---

*Permanent address: Department of Spectroscopy, University of Latvia, LV 1586 Riga, Latvia.

1050-2947/95/51(1)/231(8)/$06.00

II. EXPERIMENTAL PROCEDURE AND RESULTS

The experimental setup, shown in Fig. 1, has been described previously by Hanstorp and Gustafsson in connection with a similar high-resolution experiment where the electron affinity of iodine was determined [13]. In this experiment, negative chlorine ions were formed from HCl gas on a hot LaB_6 surface. The ions were accelerated to 3 keV, mass selected in a sector magnet and focused by means of several Einzel lenses. In an analyzing chamber, the ions were merged with a laser beam between two electrostatic quadrupole deflectors placed 50 cm apart. An ion current of typically 6 nA for ^{35}Cl and 2 nA for ^{37}Cl was measured with a Faraday cup placed after the second quadrupole deflector. The laser light could be directed either parallel or antiparallel with respect to the ion beam direction. Fast neutral atoms produced in the photodetachment process were not affected by the second quadrupole deflector. Instead, they impinged on a glass plate coated with a conductive layer of tin doped indium oxide (In_2O_3 : Sn). Secondary electrons produced by the neutral atoms were collected with a channel electron multiplier (CEM) operating in pulse counting mode. The CEM was carefully shielded, both mechanically and electrically, to prevent stray electrons from reaching the detector [14].

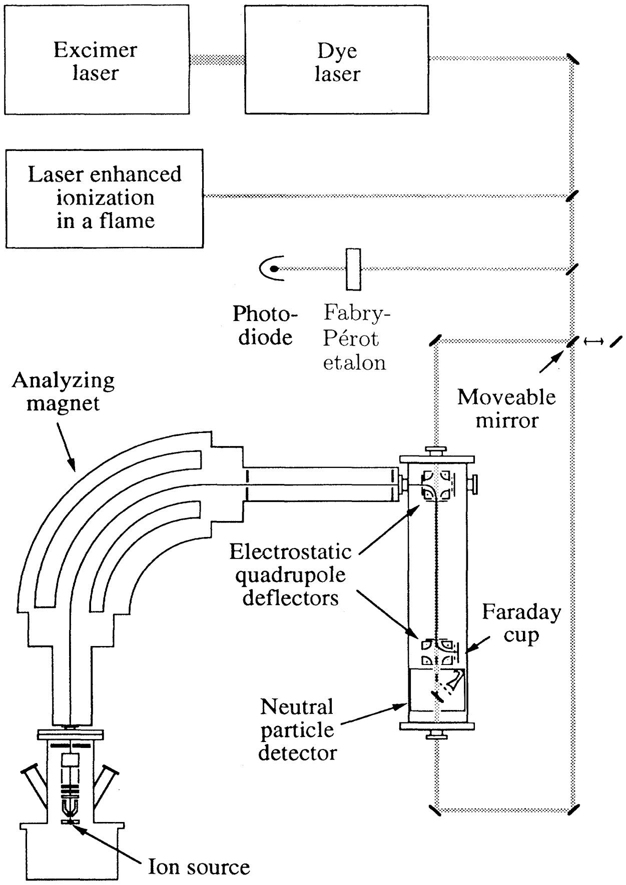

FIG. 1. Experimental set-up.

An excimer pumped dye laser served as light source. The experiment was done using two different laser dyes, BMQ (Lambdachrome No. 3570) and PTP (Lambdachrome No. 3400), with their peak intensities at 343 and 357 nm, respectively. The laser pulses, with a time duration of 20 ns, had an energy of up to 1 mJ as measured in front of the experimental chamber. Some of the laser light was directed through a Fabry-Pérot étalon and through an acetylene-air flame for wavelength calibration.

A. Detection of the photodetachment threshold

According to the Wigner law [15], the cross section for photodetachment of an *s* wave electron is, in the vicinity of the threshold, given by the expression

$$\sigma(E) = \begin{cases} c\sqrt{E - E_0}, & E \geq E_0, \\ 0, & E < E_0 \end{cases} \tag{1}$$

where $\sigma(E)$ is the cross section for photodetachment, E is the photon energy, E_0 is the photodetachment threshold, and c is a constant. The cross section behavior is, however, complicated by the hyperfine structure. The two chlorine isotopes both have a nuclear spin of 3/2. The ground state of the chlorine atom, which has the configuration $3p^5\ ^2P_{3/2}$, is therefore split into four hyperfine structure levels $F = 0$, 1, 2, and 3, where the $F = 0$ level has the lowest energy. The ground-state configuration of the negative chlorine ion, $3p^6\ ^1S_0$, shows neither fine nor hyperfine structure. With one initial state and four possible final states there are four independent photodetachment channels, which all have to be included in the fitting procedure. The relative cross section for the different channels is proportional to the multiplicity of the final state in the neutral atom, i.e., proportional to $2F + 1$, and the total photodetachment threshold can therefore be described by the function

$$\sigma(E) = c \sum_{F=0}^{3} (2F + 1) \sqrt{E - \left(E_0 + E_{hfs}^F\right)}, \quad E \geq E_0 \tag{2}$$

where E_{hfs}^F is the F dependent energy correction due to the hyperfine interaction [16], E_0 the threshold energy for leaving the atom in the lowest hyperfine level of the ground state in the atom, and c is a constant.

The nonzero bandwidth B of the laser also has to be taken into account in the evaluation procedure. In our case, we assume a Gaussian intensity distribution $I(E')$ with its peak at $E' = 0$ given by the expression [17]

$$I(E') = \tfrac{1}{2} \exp\left[-4\left(\frac{E'}{B}\right)^2\right]. \tag{3}$$

Including this bandwidth into the fitting procedure, the experimental values can be fitted to the following modified Wigner law function:

$$\sigma(E) = C \int_{E'=-\infty}^{\infty} \sum_{F=0}^{3} I(E')\,(2F+1) \sqrt{\left[E + E' - \left(E_0 + E^F_{hfs}\right)\right] + \left|E + E' - \left(E_0 + E^F_{hfs}\right)\right|}\,dE'. \quad (4)$$

The term inside the absolute sign is included in order to make the function equal to zero below the threshold. The experimental data points were fitted to Eq. (4) using a nonlinear fitting routine based on the Levenberg-Marquardt method [18]. An example of such a fit is shown in Fig. 2. Although Eq. (4) is complicated, only the constant C and the threshold energy E_0 are varied to fit the data. The two Fabry-Pérot peaks closest to the threshold, shown in the upper part of Fig. 2, were fitted to an Airy function by the same numerical method, and their positions served as frequency reference markers.

To determine the laser bandwidth, the expression in Eq. (4) was fitted to one set of experimental data for different values of the laser bandwidth. The standard deviation of those fits varied smoothly with energy, with a minimum at a bandwidth of 4.3 GHz. This value agrees with the laser specification and was used for all subsequent evaluations.

In order to correct for the first-order Doppler shift, which is sufficient in this experiment, the electron affinity $E_{EA}\left({}^{A}\text{Cl}\right)$ of the isotope ^{A}Cl is obtained as the average value of the energy of the photodetachment threshold, E_{th} obtained with parallel and antiparallel laser and ion beams (designated p and a, respectively):

$$E_{EA}\left({}^{A}\text{Cl}\right) = \frac{E^a_{th} + E^p_{th}}{2}. \quad (5)$$

B. Isotope shift

The isotope shift of the electron affinity in the negative chlorine ion has been experimentally determined by measuring the difference in electron affinity for the two stable chlorine isotopes, each determined as described in Sec. II A.

The frequency shift corresponding to the difference in electron affinity, as shown in Fig. 3, is given by the equation

$$\Delta E_{EA} = E_{EA}\left({}^{37}\text{Cl}\right) - E_{EA}\left({}^{35}\text{Cl}\right). \quad (6)$$

Alternatively, this shift can be obtained by combining Eqs. (5) and (6) giving the expression

$$\Delta E_{EA} = \frac{\Delta E^a_{th} - \Delta E^p_{th}}{2} = \frac{\left[E^a_{th}\left({}^{37}\text{Cl}\right) - E^a_{th}\left({}^{35}\text{Cl}\right)\right] - \left[E^p_{th}\left({}^{35}\text{Cl}\right) - E^p_{th}\left({}^{37}\text{Cl}\right)\right]}{2}. \quad (7)$$

Experimentally, this has the advantage that two pairs of thresholds situated very close to each other are compared, making the laser scans much shorter.

Four threshold measurements are thus required for one determination of the difference in the electron affinities of the two isotopes, ΔE_{EA}. In the present work, we performed a total of 13 isotope-shift determinations, giving an experimental value

$$\frac{\Delta E_{EA}}{h} = 0.34(14)\ \text{GHz}. \quad (8)$$

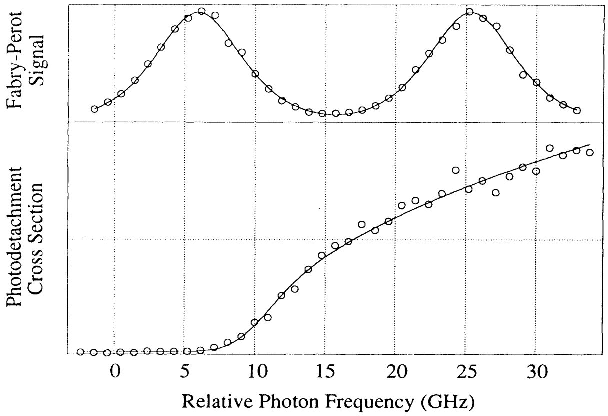

FIG. 2. A scan used in the isotope-shift measurement. The lower curve is the relative cross section for photodetachment where the line is a fit to the experimental data. The upper curve is the transmission through a Fabry-Pérot étalon used for frequency calibration.

Since the experimental results are obtained by comparing the energy of different thresholds, they are independent of an absolute wavelength calibration. Many systematic effects will therefore cancel in the evaluation procedure, giving a very high accuracy of the experimental result.

The electron affinity is defined from the threshold energy, and thus involves the difference between the ground state of the negative ion and the lowest hyperfine level of the ground state of the atom, whereas the isotope shift is normally defined as the difference between the fine-structure levels unperturbed by the hyperfine interaction. In order to extract the isotope shift from the experimental shift ΔE_{EA} in Eq. (8), it is necessary to correct for the energy difference, $\Delta E^F_{hfs} = h\delta\nu^F_{hfs}$, between the lowest hyperfine-structure level of the Cl atom and the fine-structure level unperturbed by the hyperfine structure. In ^{35}Cl, the $F = 0$ ground-state level is situated $\delta\nu^F_{hfs}\left({}^{35}\text{Cl}\right) = 0.700$ GHz below the unperturbed level and the corresponding shift in ^{37}Cl is $\delta\nu^F_{hfs}\left({}^{37}\text{Cl}\right) = 0.586$ GHz. These shifts are illustrated in Fig. 4 and were obtained using the Casimir formula, where the A and B hyperfine constants were taken from Fuller [16]. Subtracting the difference between these two values from ΔE_{EA} gives a corrected isotope shift of the electron affinity of Cl:

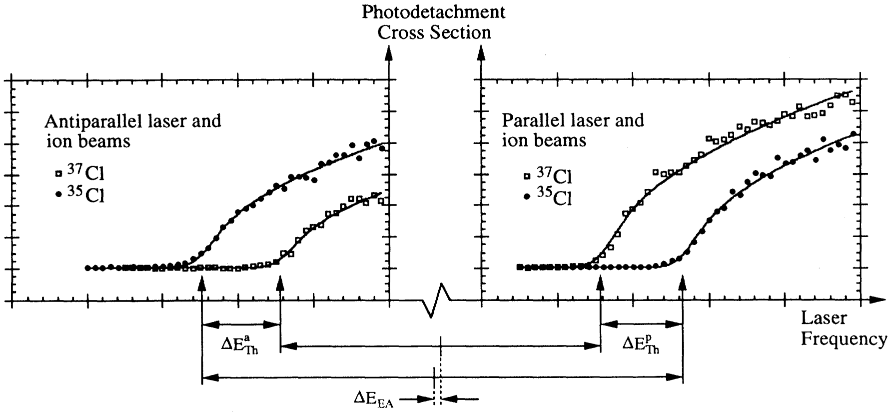

FIG. 3. A graphic description of the evaluation of the isotope shift from four different experimentally determined photodetachment thresholds.

$$\delta\nu_{IS} = \frac{\Delta E_{EA}}{h} + \delta\nu^{F}_{hfs}\,(^{37}\mathrm{Cl}) - \delta\nu^{F}_{hfs}\,(^{35}\mathrm{Cl}) = 0.22(14)\ \mathrm{GHz}. \qquad (9)$$

C. Electron affinity

In addition to the isotope-shift measurements, an improved absolute value of the electron affinity of ^{35}Cl have been determined. Extended descriptions of the experimental procedure for this experiment has been given elsewhere [13,19].

The laser wavelength was scanned between 343.7 and 344.7 nm in steps of 0.0005 nm. At each wavelength the signals from 30 laser pulses were averaged. In total seven scans, one of which is shown in Fig. 5, were recorded. Three different signals were registered, namely, the number of atoms neutralized in the photodetachment process, laser-enhanced ionization of nickel in an acetylene-air flame [20], and the transmission through a Fabry-Pérot étalon. The direction of the laser beam was reversed in the middle of the scans in order to acquire the threshold position for both the parallel and the antiparallel laser-ion beam geometries in each scan. The threshold positions were evaluated using the method described in Sec. II A. The resonant absorption lines in nickel were fitted to Lorentzian functions in order to find their peak positions. The Fabry-Pérot étalon fringes served as frequency markers in order to connect the threshold energies with the reference lines. The electron affinity, corrected for the Doppler shift, was determined by taking the mean value of the energies for the parallel and antiparallel photodetachment thresholds, as shown in Eq. 5.

The energies of the nickel reference lines have recently been measured using Fourier-transform spectroscopy [21], and they are known to within 10^{-3} cm^{-1}. As previously mentioned, we use laser-enhanced ionization in a flame in order to detect these lines [20]. The main sources of uncertainty in our calibration procedure are broadening and shifts caused by collisions in the flame.

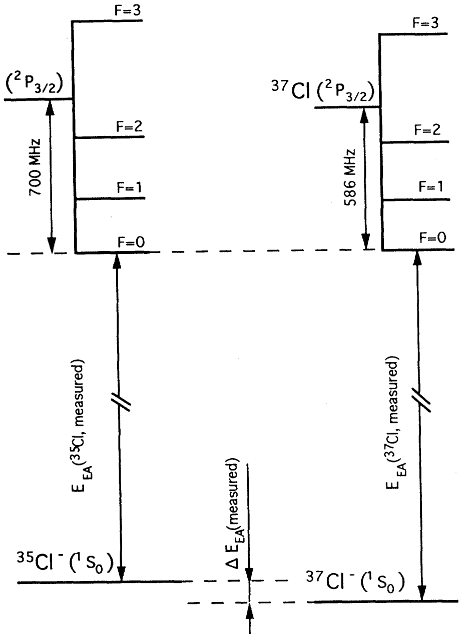

FIG. 4. The energy level diagram of the ground states of Cl$^-$ and Cl. The zero energy is set to the lowest hyperfine level in the atomic ground states of the two isotopes.

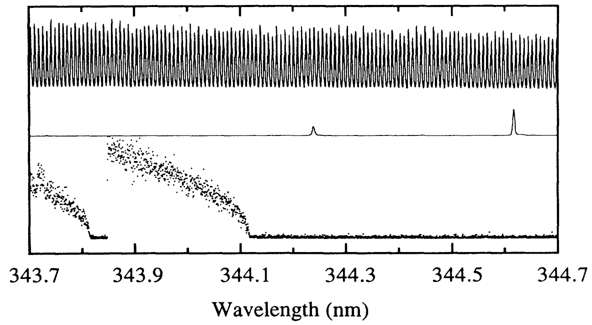

FIG. 5. A complete recording of a spectrum used for determination of the electron affinity. The lower curve is the relative photodetachment cross section, the middle curve is laser-enhanced ionization of nickel in a flame, and the upper curve is the transmission through a Fabry-Pérot étalon. The direction of the laser beam was reversed at approximately 343.85 nm.

Spectral lines are at the most redshifted with 1/3 of the pressure broadening, and experimentally observed shifts are normally smaller [22]. The widths of the spectral line profiles that we observed were approximately 11 GHz. When the contribution from the laser bandwidth and the Doppler broadening has been taken into account, a remaining pressure broadening of 10 GHz was obtained. We therefore estimate the redshift of our reference lines to be smaller than 3.3 GHz. Isotope shifts of the nickel reference lines have been measured [23] but are too small to influence our measurements.

The statistical scattering in this measurement is only 0.013 cm^{-1}. This corresponds to 0.4 GHz, which is less than one tenth of the laser bandwidth. In the error in our final result of the electron affinity, we include two standard deviations of the statistical uncertainty plus the maximum possible systematic shift due to the calibration procedure. This results in an electron affinity of $E_{EA}/hc = 29\,138.59(22)\ \text{cm}^{-1}$, which is within the uncertainty of the previously reported most accurate value 29 138.3(5) cm^{-1} [24], and an improvement of the accuracy with a factor of 2. Further, it is within the uncertainty of the result of 29 138.9(7) cm^{-1} which we recently reported [19]. In the present investigation, we have used more accurately known atomic reference lines which lie closer to the photodetachment thresholds, and we have improved the statistics. The Ni reference lines used in this investigation are $(3d^84s^2\ {}^3F_4 - 3d^84s4p\ {}^5F_4)$ at 29 084.455(1) cm^{-1} and $(3d^94s\ {}^3D_3 - 3d^94p\ {}^3F_3)$ at 29 115.975(1) cm^{-1}. All these values of the electron affinity of chlorine agree within their uncertainties, but they are outside the error bars of the value of 29 173(24) cm^{-1} recommended by Hotop and Lineberger in their compilation of atomic electron affinities [25]. With three additional determinations of the electron affinity of chlorine, it should be possible to give a more accurate recommended value.

III. ISOTOPE-SHIFT CALCULATIONS

The different nuclear masses and charge distribution of ^{35}Cl and ^{37}Cl leads to a shift in the electron affinity which can be written as [26]

$$\delta\nu_i^{A,A'} = K_i^{MS}\frac{M_A - M_{A'}}{(M_{A'} + m_e)\,M_A} + F_i(1-\kappa)\delta\left\langle r^2\right\rangle^{A,A'}, \tag{10}$$

where the first term is the mass shift accounting for the nuclear motion and the second term is the field shift arising from the change in electrostatic potential from the nucleus due to the change in charge distribution. For light elements, like Cl, the mass shift dominates. It falls off rapidly with nuclear mass, whereas the field shift increases for heavy elements, since the orbitals become more contracted and the nucleus more extended. The small correction for the field isotope shift is discussed in Sec. III B.

The expression for the mass shift factor is found by expanding the nuclear kinetic energy in Eq. (10) as $\mathbf{p}_N^2/2M_A = \left(\sum_i \mathbf{p}_i\right)^2/2M_A = \left(\sum_i \mathbf{p}_i^2 + \sum_{i\neq j}\mathbf{p}_i\cdot\mathbf{p}_j\right)/2M_A$. We find that the mass shift factor can be divided into two terms, $K^{MS} = K^{NMS} + K^{SMS}$, where the first term $K^{NMS} = m_e\nu$ gives the "normal" mass shift, and accounts for the effect of substituting the electron mass $m_e = 5.4858\times10^{-4}$ u by the reduced mass $\mu = m_eM/(m_e+M)$ in the Schrödinger equation. For the electron affinity of Cl, $K^{NMS} = 479.43$ GHz u. The mass shift between the two Cl isotopes is obtained by multiplication of the mass shift factor, K^{MS}, with the mass factor $(M_{37}-M_{35})/[M_{35}(M_{37}+m_e)] \approx 0.001\,55\ \text{u}^{-1}$, giving $\delta\nu^{NMS} = 0.74$ GHz. The nuclear masses $M_{35} = 34.96$ u and $M_{37} = 36.96$ u are obtained by subtracting $17m_e$ from the atomic masses.

The second part, $K^{SMS} = \Delta\langle\sum_{i\neq j}\mathbf{p}_i\cdot\mathbf{p}_j\rangle/h$, involves two electrons simultaneously and describes a correlation between the electronic momenta arising through the motion of the nucleus. Here, we use this nonrelativistic operator, although the orbitals used for the evaluation were obtained relativistically. The theoretical results are presented in terms of K^{SMS} in order to facilitate comparison between results for different elements.

A. The specific mass shift

The observable shift in the electron affinity results from the change in this expectation value between the closed-shell ground state of Cl$^-$ and the ground state of the neutral system with its $3p_{3/2}$ hole. This can be described using essentially the same formalism as developed for systems with one valence electron outside a closed shell, although the correlation between a hole and the core tends to be more important. In this work, however, we have included only lowest-order correlation effects, using direct summation of numerical relativistic basis functions obtained using the methods described by Salomonson and Öster [27]. This method has been applied to SMS calculations for Cs, Tl [7], and Yb$^+$ [28] and the generalization to a hole state follows that used in the nonrelativistic calculation for the shift of the binding energy of Ne [6].

For scalar operators, like the SMS, the core gives very large contributions (≈ -144 THz u in this case), which, however, cancel between initial and final states. An advantage of perturbation theory is the cancellation of contributions from the unperturbed core automatically obtained by omitting the "zero-body" terms describing these contributions. In the case of a single hole state only "one-body" terms need to be evaluated.

The first contribution to K^{SMS} is the interaction of the hole with all core electrons. Only the exchange terms contribute to the expectation value, making the first-order value negative. Evaluating the expectation value between Dirac-Fock (DF) orbitals for the ground state of Cl$^-$, which is used as a reference, gives -3.68 THz u. The DF value is a sum over the interactions of the $3p_{3/2}$ with all core orbitals whose l-quantum number differs by one unit and j value differs by at most one unit from the values of the hole, i.e., all the ns electrons. The interaction with $1s$ electrons is found to dominate, giving -2.24 GHz u—the smaller overlap is compensated by the larger momenta of the inner core electrons.

The ionization of Ne, studied in earlier work [6], involves the removal of a $2p_{3/2}$ electron. In that case, the DF contribution to the mass shift constant, K^{SMS}, is -9.00 THz u, of which the $1s$-$2p$ interaction accounts for -8.24 THz u. In spite of the larger nuclear charge of Cl, which leads to increased electronic momenta, the higher principal number of the active electron in Cl leads to a smaller DF value for K^{SMS}.

The nuclear motion affects the wave function of *all* electrons, thereby modifying, e.g., the interaction between the core and the $3p$ hole. The change in the $3p$ energy due to the first-order correction of the core gives a contribution 4.77 THz u to the SMS constant, i.e., larger than the DF value but with opposite sign. However, these orbital corrections affect also the interactions within the core. A self-consistent treatment of the core orbital modifications, closely related to the "random-phase approximation" (RPA) approach, reduces the orbital modification effect by about 40%, to 2.83 THz u. Adding this value to the DF contribution cancels a large part of it, leaving a sum of only -0.84 THz u. We note that Bauche [29], in his pioneering nonrelativistic isotope-shift calculations, performed separate Hartree-Fock calculations for the initial and final states and in this way include automatically the "RPA" terms. Also for the shift of the ionization energy in Ne, the orbital modifications give significant reduction of the mass shift constant, although the corrections for an atom are not quite as drastic as for a negative ion, where the interaction between the electrons plays a more dominant role. The first-order modification gives 8.72 THz u, changed to 5.43 THz u by the self-consistent treatment. Figure 6 shows the theoretical results at different levels of approximation for these two systems, together with the experimental values.

Being a two-particle operator the SMS is very sensitive to correlation effects, which arise already in second order where they were found to give 1.17 THz u, thereby changing the overall sign, giving $K^{SMS} = 0.32$ THz u, corresponding to a shift between the two stable Cl isotopes of 0.50 GHz. In view of the large cancellations, this result is very uncertain. For Ne, the lowest-order correlation effect, 2.04 THz u, leads to a theoretical value -1.54 THz u, compared to the experimental value -2.4 THz u. Higher-order effects must thus reduce the correlation contribution for Ne. Lowest-order correlation effects, in fact, often give an overestimate, as pointed out, e.g., by Dzuba *et al.* [30], who advocate the use of a screened Coulomb potential to describe the electron correlation. The modification of the valence orbital to an approximate Brueckner orbital is often a very important correlation effect [31]. Here, we evaluated these corrections to lowest order, and found a reduction of the DF and RPA results of only about 1.4 %. A more complete treatment of higher-order correlation effects would be essential to obtain agreement with experimental data.

B. The field isotope shift

In addition to the mass-dependent isotope shift described above, a shift in the electron affinity can also arise due to changes $\delta\langle r^2\rangle^{35:37}$ in the nuclear charge distribution, as shown in Eq. (10). The electronic factor F for the field shift is given by

$$F = -4\pi\Delta\,|\Psi(0)|^2\,\frac{Z}{6}\,\frac{e^2}{4\pi\varepsilon_0} \tag{11}$$

and is determined by the change in electron density, $|\Psi(0)|^2$, at the nucleus between the lower and upper state of the transition. The $3p_{3/2}$ electron, itself, has a negligible density at the nucleus. Nevertheless, its removal causes a change in the distribution of the s electrons in the core. Including these RPA-type corrections to first order gives $F \approx 254$ MHz/fm^2. Similar to the SMS, a self-consistent treatment of the RPA terms gives a significant reduction: $F \approx 117$ MHz/fm^2. We note that this value is comparable to the factor $F_{4s}(K) \approx -103$ MHz/fm^2 for the binding energy of the $4s$ ground state of the nearby alkali-metal atom K, but is considerably larger than the factor for its first p state $F_{4p}(K) \approx 4.6$ MHz/fm^2.

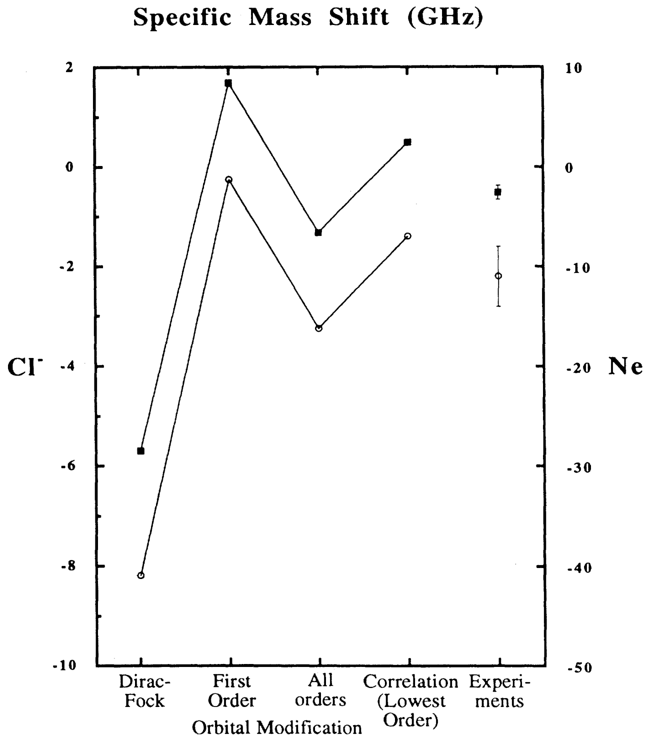

FIG. 6. A comparison between the experimental value for the specific mass shift for the electron affinity in Cl and theoretical results at different levels of approximation. For comparison, the corresponding results are also shown for the shift of the ionization potential of Ne (with the scale to the right). The first value is evaluated using orbitals obtained in the Dirac-Fock potential from the unperturbed closed-shell core and the next two values show, respectively, the lowest-order and all-order effect of the modification of the core orbitals due to the removal of an np electron. The final theoretical value accounts also to lowest (i.e., second) order for the correlation effects and involves the simultaneous excitation of two electrons (GHz).

The correction term κ in Eq. (10) accounts for higher moments, $\delta\langle r^4\rangle$, $\delta\langle r^6\rangle,\ldots$, of the nuclear charge distribution, but is negligibly small (about 0.4%) for Cl.

Briscoe *et al.* [32] have measured the charge distributions of ^{35}Cl and ^{37}Cl using electron scattering. From their parameters for the Fermi distribution, we obtain $\delta\langle r^2\rangle^{35:37} = 0.12(12)$ fm^2. Combining this result with our calculated F value indicates that the field isotope shift of the electron affinity $\delta\nu_{FS}^{35:37} = 14(14)$ MHz, which is well below the error bars of the isotope-shift measurement.

IV. COMPARISON BETWEEN THEORY AND EXPERIMENT

The experimentally determined difference between electron affinity for the two naturally occurring chlorine isotopes of the fine-structure levels unperturbed by the hyperfine interaction was $\Delta\nu_{IS} = 0.22(14)$ GHz, as discussed in Sec. II B.

Subtraction of the normal mass shift (see Sec. III)

$$\delta\nu_{NMS} = \frac{\nu m_e \Delta M}{M_{35}M_{37}} = 0.74 \text{ GHz}$$

gives a "residual shift" of $-0.51(14)$ GHz. As seen in Sec. III B, the field shift is only $\delta\nu_{FS} = 14(14)$ MHz, leaving a specific mass shift of

$$\delta\nu_{SMS} = -0.51(14) \text{ GHz}$$

corresponding to a factor $K_{SMS} = -0.33(9)$ THz u. This value is close to the theoretical result, but with opposite sign.

In order to understand better the cause of this apparent contradiction, we show in Fig. 6 the results obtained at various levels of approximation. The final result arises from large cancellation. The DF expectation value is many times larger than the final result. The lowest-order orbital modification ("RPA terms") is of comparable size and with opposite sign. Higher-order RPA terms cancel about 40% of the first-order orbital modification correction. It seems like the lowest-order correlation effects are overestimated by a similar amount: the experimental value is about halfway between the result with and without lowest-order correlation. For comparison we show in Fig. 6 also the experimental [12] and analogous theoretical values [6] for the specific mass shift in the ionization potential of neon. The calculated specific mass shift for neon is -7 GHz, whereas the experimental value is -11.3 GHz. Although slightly outside the uncertainty of the experimental value, the theoretical value in this case has the right sign. The negative first-order DF value plays a more dominant role for an atom than for a negative ion.

Similar results are obtained for the chlorine electron affinity, itself: The DF value, 0.1480 a.u., is about 11% larger than the experimental value 0.1328 a.u., but the lowest-order correlation effects bring a reduction of about 20%, giving a theoretical value of 0.1181 a.u., again demonstrating the need for more complete treatment of correlation effects. The coupled-cluster approach provides a systematic procedure for including higher-order effects [33], which has given quite accurate results for systems with one valence electron [34], and could be applied also to hole states, although that has not yet been implemented in our program.

V. CONCLUSION

We have determined the isotope shift in the electron affinity of Cl to be 0.22(14) GHz, of which $-0.51(14)$ GHz is due to the specific mass shift. This is to our knowledge the highest resolution obtained in any laser experiment on atomic negative ions, and the resolution is even higher than in electron-affinity determinations where single-mode dye lasers have been used [35]. This could be achieved since an isotope-shift measurement involves comparison of photodetachment thresholds, rather than an absolute determination. Many systematic uncertainties will therefore cancel, giving a very high accuracy in the experimental result. Further, the collinear geometry in combination with the high photon flux from the pulsed dye laser gives a very good counting statistics.

Experimentally it would be very hard to improve the resolution on the isotope shift on chlorine since the measured shift is only 1/30 of the bandwidth of the laser. A more precise experiment could, however, be made using a negative ion where the photodetachment threshold corresponds to the wavelength region of a single-mode dye laser. The laser light should then be amplified in a pulsed amplifier in order to keep the good signal to background ratio obtained in the present experiment. S$^-$ could then be a suitable choice, although it would probably be necessary to use isotopically enriched sulfur. The theoretical treatment of such a system is more complicated, but might be amenable to multiconfiguration Hartree-Fock calculations [36,37]. Investigating a few-electron system, like Li$^-$, would give more insight, since very accurate calculations could be performed. In this case, however, the experimental conditions are much more unfavorable. Nevertheless, the experimental accuracy in the shift of the electron affinity of Cl is sufficient to demonstrate the importance of higher-order correlation effects.

Finally, we conclude that this is the third experiment showing an electron affinity of chlorine deviating from the currently recommended value. A more precise recommendation of this quantity could therefore be given by means of this and previous experiments.

ACKNOWLEDGMENTS

We would like express our appreciation to O. Axner, who lent us the laser system used in the experiment. Financial support by the Swedish Natural Science Research Council is gratefully acknowledged. The visit by U.B. was made possible by financial support from the Swedish Institute and from the International Research Fund at Göteborg University.

[1] S. Salomonson and P. Öster, Phys. Rev. A **41**, 4670 (1990).

[2] S. Geltman, Phys. Rev. A **42**, 6958 (1990).

[3] M. L. Du, Phys. Rev. A **40**, 1330 (1989).

[4] M. Vincke and D. Baye, J. Phys. B **22**, 2089 (1989).

[5] A.-M. Mårtensson and S. Salomonson, J. Phys. B **15**, 2115 (1982).

[6] S. Hörbäck, A.-M. Mårtensson-Pendrill, S. Salomonson, and U. Österberg, Phys. Scr. **28**, 469 (1983).

[7] A. Hartley and A.-M. Mårtensson-Pendrill, J. Phys. B **24**, 1193 (1991).

[8] K. R. Lykke, K. K. Murray, and W. C. Lineberger, Phys. Rev. A **43**, 6104 (1991).

[9] P. A. Schulz, R. D. Mead, P. L. Jones, and W. C. Lineberger, J. Chem. Phys. **77**, 1153 (1982).

[10] G. Herzberg, Proc. R. Soc. London Ser. A **248**, 309 (1958).

[11] S. A. Aseyev, Y. A. Kudryavtsev, V. S. Letokhov, and V. V. Petrunin, J. Phys. B **24**, 2755 (1991).

[12] W. B. Westerveld and J. van Eck, J. Phys. B **12**, 377 (1979).

[13] D. Hanstorp and M. Gustafsson, J. Phys. B **25**, 1773 (1992).

[14] D. Hanstorp, J. Meas. Sci. Tech. **3**, 523 (1992).

[15] E. P. Wigner, Phys. Rev. **73**, 1002 (1948).

[16] G. H. Fuller, J. Phys. Chem. Ref. Data **5**, 835 (1976).

[17] W. Demtröder, *Laser Spectroscopy* (Springer-Verlag, Berlin, 1982).

[18] W. H. Press, B. P. Flannery, S. A. Teukolsky, and W. T. Vetterling, *Numerical Recipies* (Cambridge University Press, Cambridge, England, 1986).

[19] D. Hanstorp, M. Gustafsson, U. Berzinsh, and U. Ljungblad, Nucl. Instrum. Methods B **79**, 159 (1993).

[20] O. Axner *et al.*, J. Appl. Phys. **55**, 3215 (1984).

[21] U. Litzen, J. W. Brault, and A. P. Thorne, Phys. Scr. **47**, 628 (1993).

[22] H. C. Wagenaar and L. de Galan, Spectrochim. Acta B **28**, 157 (1973).

[23] D. J. Schroeder and J. E. Mack, Phys. Rev. **121**, 1726 (1961).

[24] R. Trainham, G. D. Fletcher, and D. J. Larson, J. Phys. B **20**, L777 (1987).

[25] H. Hotop and W. C. Lineberger, J. Phys. Chem. Ref. Data **14**, 731 (1985).

[26] W. H. King, *Isotope Shifts in Atomic Spectra* (Plenum Press, New York, 1984).

[27] S. Salomonson and P. Öster, Phys. Rev. A **40**, 5548 (1989).

[28] A.-M. Mårtensson-Pendrill, D. S. Gough, and P. Hannaford, Phys. Rev. A **49**, 3351 (1994).

[29] J. Bauche, J. Phys. (Paris) **35**, 19 (1974).

[30] V. A. Dzuba, V. V. Flambaum, P. G. Silvestrov, and O. P. Sushkov, Phys. Lett. A **131**, 461 (1988).

[31] I. Lindgren, J. Lindgren, and A.-M. Mårtensson, Z. Phys. A **279**, 113 (1976).

[32] W. J. Briscoe, H. Crannell, and J. C. Bergstrom, Nucl. Phys. A **344**, 475 (1980).

[33] I. Lindgren, Int. J. Quantum Chem. Symp. **12**, 33 (1978).

[34] S. Salomonson and A. Ynnerman, Phys. Rev. A **43**, 88 (1991).

[35] D. M. Neumark, K. R. Lykke, T. Andersen, and W. C. Lineberger, Phys. Rev. A **32**, 1890 (1985).

[36] C. Froese Fischer, Comput. Phys. Commun. **64**, 431 (1991).

[37] H. Schuessler *et al.*, Phys. Rev. A **45**, 6459 (1992).